Azolylpentazoles as High-Energy Materials: A Computational Study

Anton Hammerl,[a] Thomas M. Klapötke,[b] and Peter Schwerdtfeger*[a]

Abstract: The structures of highly energetic substituted pentazole compounds and their decomposition to give dinitrogen and the corresponding azide were investigated by ab initio quantum chemical methods. The substituents include azolyl groups (five-membered aromatic rings with different numbers of nitrogen atoms), CH_3, CN, and F. The decomposition pathway was followed for several substituted azolyl- and phenylpentazoles and compared to the known experimental and theoretical results. The NMR parameters of most of the as-yet unknown pentazole compounds were predicted. The activation energy for the decomposition increases, while the decomposition energy of the substituted pentazole decreases with greater electron-donating character of the substituent of the pentazole. Thus, anionic pentazoles are more stable than neutral pentazoles. Methylpentazole is predicted to be among the most stable pentazoles, even though it does not contain an aromatic system.

Keywords: ab initio calculations · nitrogen · nitrogen heterocycles · pentazoles · polynitrogen

Introduction

The large positive heats of formation of nitrogen-rich and polynitrogen compounds make them promising targets for the synthesis of highly energetic materials, as illustrated by the recent examples of 3,3′-azobis(6-amino-1,2,4,5-tetrazine)[1] and hydrazinium *N*,*N*′-azobistetrazolate.[2] The successful synthesis of N_5^+[3, 4] led to an increased interest in polynitrogen compounds,[5, 6] and to the detection of N_5^-[7] and N_4.[8, 9] Calculations have already predicted many stable polynitrogen species over the last twenty years, the best example being N_5^+.[10] Structures for neutral (N_3,[11] N_4,[12–17] N_5,[18, 19] N_6,[12, 14, 19–23] N_7,[24–26] N_8,[12, 14, 27–34] N_9,[35] N_{10},[12, 28, 32, 36–40] N_{12},[12, 32, 40, 41] N_{20}[42] and N_{60}[36]) and charged compounds (N_4^{2+},[40] N_5^-,[16, 28, 43, 44] N_6^+,[19] N_6^-,[19] N_6^{2+}[40]), pentazole HN_5,[34, 39, 45, 46] and salts of the pentazole anion[47, 48] were investigated intensively in the past. Calculations showed that N_5^- and N_7^{3-} might be stabilized as transition-metal complexes such as $Fe(N_5)_2$[49, 50] or ScN_7.[51, 52] The aromaticity of pentazole[53–55] and its electric quadrupole moment[56] were also investigated. The combination of N_5^+ with a polynitrogen anion has also been studied by quantum chemical methods.[57–60]

[a] Prof. Dr. P. Schwerdtfeger, Dr. A. Hammerl
Department of Chemistry, University of Auckland
Private Bag 92019, Auckland (New Zealand)
Fax: (+64) 3737422
E-mail: p.schwerdtfeger@auckland.ac.nz

[b] Prof. Dr. T. M. Klapötke
Department Chemie
Ludwig-Maximilians Universität München
Butenandtstr. 5-13 (D), 81377 München (Germany)
E-mail: Thomas.M.Klapoetke@cup.uni-muenchen.de

The first pentazole compounds, synthesized in 1956,[61–63] were substituted by a phenyl ring. The crystal structure of *p*-dimethylaminophenylpentazole, determined more than twenty years later,[64] and that of phenylpentazole, reported recently,[65] show that pentazole is a planar five-membered ring with almost equal N–N distances. Kinetic studies on *p*-substituted phenylpentazoles demonstrate that electron-donating substituents like NMe_2 and electron-withdrawing substituents such as NO_2 respectively increase and decrease the stability of pentazole with respect to decomposition.[66, 67] Studies by NMR spectroscopy gave accurate kinetic data for the decomposition and proved that the pentazole ring is relatively stable in solution.[68–70] The correct mechanism for the formation and decomposition of phenylpentazole was determined only recently from a combined NMR and quantum chemical study.[71] It was shown that the reaction of an azide ion with a phenyl diazonium compound forms three open-chain PhN_5 compounds. One isomer (*Z*,*E*) decomposes instantly to phenylazide and dinitrogen, another (*E*,*E*) can rearrange to a third isomer (*E*,*Z*), which can also be formed directly and undergoes cyclization to form a pentazole. Decomposition follows a different mechanism: phenylpentazole is involved in a 1,3-dipolar cycloreversion with elimination of dinitrogen to form phenylazide.[71]

To help find new stable nitrogen-rich compounds and obtain a more comprehensive picture of the stability of such high-energy compounds, we studied the structure and stability of a large number of substituted pentazole compounds by ab initio quantum chemical methods. We determined the activation barrier and the energy of decomposition to the corresponding azides and N_2 [Eq. (1)]. Since recent NMR studies suggest that it is possible to attach pentazole to tetrazole,[72]

 DOI: 10.1002/chem.200305125

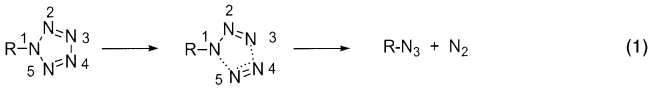

(1)

the properties of compounds in which pentazole is attached to five-membered aromatic rings containing different numbers of nitrogen atoms (azoles) were also investigated. It is well known that the acidity of azoles increases in the order pyrrole < pyrazole < imidazole < 1,2,3-triazole < 1,2,4-triazole < tetrazole < pentazole.[73] Hence, it can be assumed that pyrrole is a better electron donor than tetrazole, and pyrrolylpentazole should be thermodynamically more stable than tetrazolylpentazole, which we also investigated. We included HN_5,[68] N_5^-,[16] N_{10},[68] tetrazolylpentazole[72] and phenylpentazole[71] in our calculations so that the results could be compared with experimental data. To evaluate substituent effects we examined the decomposition of *p*-dimethylaminopentazole, *p*-nitrophenylpentazole, and amino-substitued pyrrolylpentazoles. Finally, the nonaromatic methyl-, *tert*-butyl-, and cyanopentazoles as well as fluoropentazole were investigated (Tables 1–3). For the future characterization of these compounds we produced ^{15}N NMR chemical shift data.

Table 1. Numbering scheme for substituted pentazoles RN_5 (only the group R is shown). The symmetry is given for the whole molecule.

					
C_1	C_s	C_s	C_s	C_1	C_s
1	**2**	**3**	**4**	**5**	**6**
					
C_s	C_1	C_s	C_s	C_1	C_1
7	**8**	**9**	**10**	**11**	**12**
				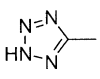	
C_s	C_1	C_s	C_s	C_1	D_{2d}
13	**14**	**15**	**16**	**17**	**18**
H	F	CH_3	CN	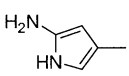	
C_{2v}	C_{2v}	C_s	C_{2v}	C_1	C_1
19	**20**	**21**	**22**	**23**	**24**

Table 2. Numbering scheme for substituted pentazoles RN_5^- (only the group R is shown). The symmetry is given for the whole molecule.

					
C_s	C_1	C_s	C_1	C_s	C_1
25	**26**	**27**	**28**	**29**	**30**
				–	
C_1	C_1	C_1	C_1	D_{5h}	
31	**32**	**33**	**34**	**35**	

Table 3. Numbering scheme for substituted phenylpentazoles *p*-$RC_6H_4N_5$ (only the group R is shown). The symmetry is given for the whole molecule.

H	NO_2	$N(CH_3)_2$
C_1	C_2	C_1
36	**37**	**38**

Results and Discussion

Minimum structures: Our calculated geometries of the pentazole ring systems agree well with the values from X-ray diffraction and calculations by other groups (Table 4). Larger deviations are only found for Hartree–Fock calculations on FN_5[45] and CH_3N_5,[46] and this underlines the necessity of including electron correlation.[6, 20] As expected, the pentazole ring is planar with almost equal N–N bond lengths of about 1.32 Å, the N3–N4 bond always being longer than the other N–N bonds by about 0.02 Å. It is interesting that the variety of different substituents, from electron-withdrawing (**20**, **37**) to electron-donating (azolylpentazoles, anions), hardly affect the geometry of the ring system. For example, the 1*H*-pyrrolyl compound **2** and the amino-substituted 2*H*-pyrrolyl compound **24** have almost identical bonding parameters in the pentazole ring. All azolylpentazole compounds have low rotational barriers around the C–N single bond involving N1 of the pentazole ring. For most compounds the minimum structure is not planar, that is, the ring systems are twisted, and the completely planar structure represents a transition state. For example, at the MP2 level planar D_{2h} N_{10} lies 4.6 kcal mol^{-1} above the minimum D_{2d} structure,[13, 21, 36] and this compares well with a previous result (3.2 kcal mol^{-1} at the MP2(FC)/cc-pVDZ level[36]). All other rotational transition states are less than 1.2 kcal mol^{-1} (**33**) above the minimum structure at the MP2 level. Figure 1

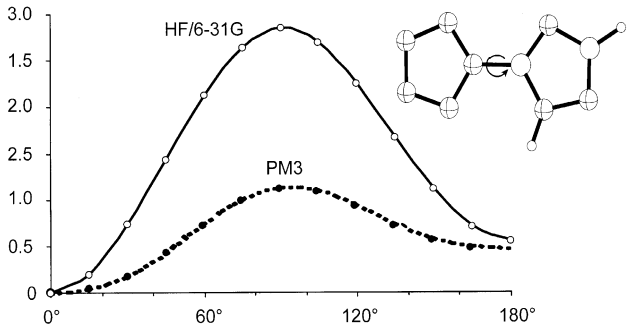

Figure 1. Rotation of **13** around the C–N single bond between the rings (the angle between the ring planes is plotted against the relative energy in kcal mol^{-1}). For comparison, results obtained from a semi-empirical method (PM3)[84] are also given.

shows the change in energy for rotation about the C–N bond of **13**. The angle between ring planes of the nonplanar C_1 pentazoles is close to either 30 or 60°, and **18** has the maximum angle of 90°. The amino-substituted pentazole **23** is almost planar (3.5°), and **24** has an angle of 21.5° between the ring planes. For the azolylpentazolates **25**–**34** the angle between the ring planes for the C_1 structures is between 22

Table 4. Optimized geometries of the pentazole ring system for selected pentazole compounds [bond lengths in Å and angles in degrees].

	2	**13**	**18**	**18**[a]	**19**	**19**[b]	**20**	**21**	**24**	**26**
N1–R1	1.400	1.405	1.348	1.344	1.011	1.014	1.322	1.453	1.402	1.411
N1–N2	1.330	1.330	1.334	1.322	1.322	1.324	1.311	1.325	1.331	1.335
N2–N3	1.322	1.319	1.309	1.304	1.318	1.321	1.325	1.320	1.322	1.329
N3–N4	1.335	1.339	1.355	1.344	1.342	1.344	1.343	1.339	1.336	1.332
N4–N5	1.323	1.320	1.309	1.304	1.318	1.321	1.325	1.320	1.322	1.327
N1–N5	1.328	1.329	1.334	1.322	1.322	1.324	1.311	1.325	1.331	1.336
N1-N2-N3	104.2	104.1	103.1	–	103.7	103.7	101.9	104.4	104.2	104.5
N2-N3-N4	109.3	109.2	109.8	109.7	109.4	109.4	109.7	109.2	109.5	109.6
N3-N4-N5	109.6	109.9	109.8	109.7	109.4	109.4	109.7	109.2	109.2	109.2
N4-N5-N1	104.0	103.6	103.1	–	103.7	103.7	101.9	104.4	104.5	104.8
N2-N1-N5	112.9	113.3	114.3	114.5	113.9	113.9	116.9	112.9	112.5	112.0
N2-N1-R1	122.7	121.3	122.9	122.8	123.0	123.1	121.5	123.5	124.1	125.2
N5-N1-R1	124.4	125.4	122.9	122.8	123.0	123.1	121.5	123.5	123.4	122.8
	33	**35**	**35**[c]	**36**	**36**[d]	**36**[e]	**37**	**37**[f]	**38**	
N1–R1	1.421	–	–	1.423	1.428	1.437(5)	1.422	1.425	1.419	
N1–N2	1.33	1.336	1.329	1.331	1.338	1.32(1)	1.331	1.334	1.332	
N2–N3	1.322	1.336	1.329	1.318	1.326	1.308(2)	1.318	1.295	1.319	
N3–N4	1.338	1.336	1.329	1.340	1.347	1.337(6)	1.340	1.354	1.340	
N4–N5	1.322	1.336	1.329	1.318	1.326	1.307(8)	1.318	1.295	1.319	
N1–N5	1.33	1.336	1.329	1.331	1.338	1.322(2)	1.331	1.334	1.332	
N1-N2-N3	104.6	108.0	108.0	104.4	104.5	105.3(1)	104.3	105.2	104.4	
N2-N3-N4	109.2	108.0	108.0	109.4	109.4	108.9(1)	109.4	109.1	109.4	
N3-N4-N5	109.2	108.0	108.0	109.4	109.3	109.0(1)	109.4	109.1	109.4	
N4-N5-N1	104.6	108.0	108.0	104.4	104.5	105.3(1)	104.3	105.2	104.4	
N2-N1-N5	112.4	108.0	108.0	112.6	112.4	111.5(1)	112.7	111.3	112.5	
N2-N1-R1	123.8	–	–	123.7	123.8	124.4(1)	123.7	124.4	123.7	
N5-N1-R1	123.8	–	–	123.7	123.8	124.1(1)	123.7	124.4	123.8	

[a] MP2(FC)/cc-PVTZ.[36] [b] MP2(FC)/6-311 + G(d,p).[68] [c] CCSD(T)/aug-cc-pVTZ.[16] [d] MP2(FC)/6-31G(d).[68] [e] X ray.[65] [f] B3LYP/6-31 + G*.[70]

(**26**) and 60° (**34**), with a maximum energy difference of 1.2 kcal mol^{-1} for **34**. In contrast to the crystal structures,[64, 65] and previously calculated structures for phenylpentazoles at the MP2(FC)/6-31G[71] and B3LYP/6-31 + G(d,p) levels of theory,[70] our results give first-order transition states for the planar phenylpentazoles **36** and **37**. The energy difference between planar and twisted structures, however, is only 0.2 kcal mol^{-1} for **36** and **37**. The torsion angles between the phenyl and pentazole rings are 26.0° for **36**, 24.0° for **37** and 24.7° for **38**. No minimum structures for nitro- and nitrosopentazole were found at the MP2 level of theory because they decompose.

The azole tautomers differ in energy by no more than 3 kcal mol^{-1}; only **15** is 7.4 kcal mol^{-1} higher in energy than the lowest energy tautomer **14**. Generally the 2*H* tautomer has a lower energy than the 1*H* tautomer. This was verified recently for tetrazole in the gas phase.[74] In solution, the more polar 1*H*-tetrazole tautomer is more favoured by polar solvents,[75, 76] and in the solid state, where hydrogen bonding must be considered, only the 1*H*-tetrazole tautomer is known.[77]

Transition states and reaction paths: The transition state structures (Table 5) show lengthening of the N1–N5 and N3–N4 bonds by about 0.2 Å and shortening of the N4–N5 distance by about 0.1 Å, in accordance with a 1,3-dipolar cycloreversion. The N1–N5 distance is shorter than the N3–N4 distance, and this implies an asymmetric ring opening. For the symmetric pentazolate anion **35** we found a transition state of C_{2v} symmetry. In general, the transition state is more "symmetrical" for the phenylpentazoles **36**–**38** and more "asymmetrical" for the smaller pentazoles **19**–**22**. Interestingly, for dipentazole **18**, pentazole **19** and fluoropentazole **20** the distorted five-membered ring of the pentazole in the transition state has an envelope configuration, in which the N1 nitrogen atom lies out of the ring plane (for a comparison of the transition states, see Figures 2–4). For these transition states we obtain equal N1–N2 and N1–N5, as well as equal N2–N3 and N4–N5 distances. The change in geometry of the transition state can be attributed to the electron-withdrawing substituents.[19]

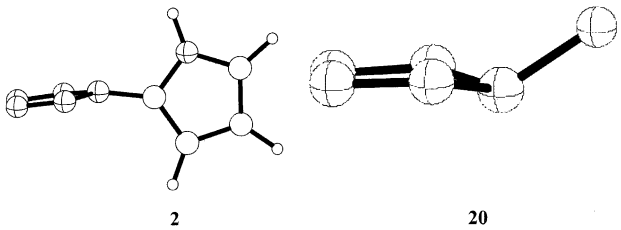

2 **20**

Figure 2. Planar and envelope ring configurations of the distorted five-membered rings in the transition states of **2** and **20**.

All transition states of azolylpentazoles have angles between the planes of the azolyl ring and the distorted five-membered ring of the pentazole of 45–75° for the azolylpentazoles and 60–90° for the anions. Benin et al. report a connection between the nature of the substituent (electron-withdrawing or -donating) and the angle between ring planes in the transition state.[70] As the larger angles for the anions

Table 5. Optimized geometrical parameters of the pentazole ring system of selected transition states [bond lengths in Å and angles in degrees].

	2	**13**	**18**	**19**	**19**[a]	**20**	**21**	**24**
N1−R1	1.388	1.397	1.350	1.017	1.020	1.357	1.458	1.397
N1−N2	1.349	1.355	1.437	1.399	1.411	1.427	1.337	1.578
N2−N3	1.217	1.216	1.208	1.199	1.202	1.213	1.212	1.196
N3−N4	1.796	1.781	1.772	1.961	1.943	1.753	1.874	1.758
N4−N5	1.197	1.199	1.208	1.197	1.202	1.213	1.194	1.226
N1−N5	1.535	1.520	1.437	1.425	1.412	1.427	1.512	1.322
N1-N2-N3	117.1	116.3	111.5	117.0	115.9	111.3	119.2	108.5
N2-N3-N4	101.0	101.4	103.6	98.0	98.7	103.4	98.4	105.9
N3-N4-N5	104.4	104.4	103.6	98.6	98.7	103.4	102.1	101.0
N4-N5-N1	110.0	110.0	111.5	115.9	115.9	111.3	112.1	118.3
N2-N1-N5	107.3	107.4	109.0	109.5	109.6	108.4	107.6	106.0
N2-N1-R1	125.5	121.2	118.3	116.4	116.4	113.9	121.3	123.7
N5-N1-R1	123.8	119.8	118.4	116.1	116.4	113.9	118.6	124.2
	26	**35**	**35**[b]	**36**	**36**[b]	**37**	**37**[c]	**38**
N1−R1	1.396	–	–	1.411	1.410	1.409	1.401	1.409
N1−N2	1.319	1.257	1.252	1.304	1.281	1.308	1.282	1.303
N2−N3	1.226	1.257	1.252	1.227	1.219	1.194	1.219	1.230
N3−N4	1.777	1.695	1.764	1.742	1.721	1.745	1.710	1.727
N4−N5	1.197	1.203	1.191	1.194	1.174	1.226	1.174	1.194
N1−N5	1.579	1.695	1.764	1.601	1.747	1.590	1.748	1.613
N1-N2-N3	119.5	126.3	128.9	118.6	122.0	107.5	121.5	118.7
N2-N3-N4	100.5	99.0	–	101.2	101.6	106.5	101.9	101.5
N3-N4-N5	105.0	107.9	–	106.8	110.3	101.3	110.9	107.2
N4-N5-N1	109.6	107.9	–	107.3	103.7	118.2	103.1	106.9
N2-N1-N5	105.4	99.0	–	105.9	102.3	106.3	102.7	105.5
N2-N1-R1	128.7	–	–	126.4	126.4	123.5	127.1	126.3
N5-N1-R1	124.8	–	–	123.8	127.6	126.1	130.3	124.1

[a] MP2(FC)/6-311 + G(d,p).[68] [b] CCSD(T)/6-311 + G(d,p).[19] [c] B3LYP/6-31 + G*.[70]

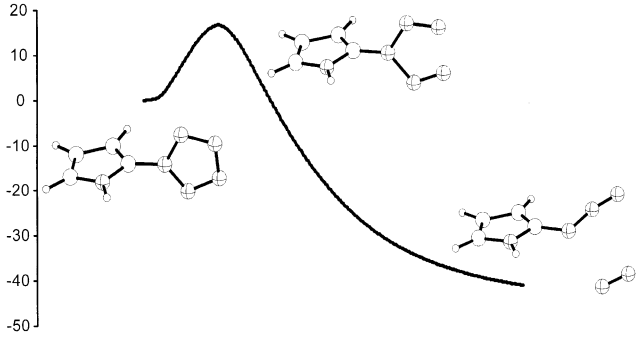

Figure 3. Reaction path for the decomposition of 1*H*-pyrrolylpentazole **2** to form 1*H*-pyrrolylazide and dinitrogen (relative energies are given in kcal mol^{-1}).

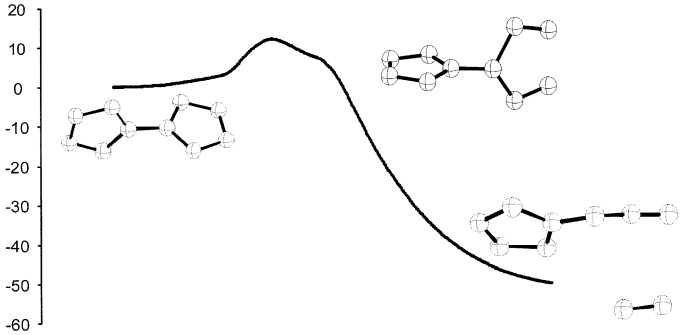

Figure 4. Reaction path for the decomposition of N_{10} (dipentazole; **18**) to form pentazole azide N_8 and dinitrogen (relative energies are given in kcal mol^{-1}).

illustrate, we find the same correlation for similar molecules (**36**: 20.5°, **37**: 14.9°, **38**: 30.4°; **37** has the most electron-withdrawing, and **38** the most electron-donating substituent).

Mulliken charges: With the exception of fluoropentazole (**20**), all pentazole N1 nitrogen atoms have negative Mulliken charges (Table 6). Here the electronegative fluoro substituent ($q = -0.17$) results in a positive charge on N1 of pentazole ($q = 0.27$) and smaller charges for all other N atoms (0.01). As expected, the negative charges at N2 to N5 in the anionic

Table 6. Mulliken charges of the pentazole ring system and the attached atom for selected pentazole compounds.

	2	**13**	**18**	**19**	**19**[a]	**20**	**21**
R1	0.625	0.844	−0.031	0.435	0.376	−0.172	−0.421
N1	−0.289	−0.311	−0.031	−0.266	−0.257	0.272	−0.122
N2	−0.057	−0.041	0.056	−0.009	0.025	0.009	−0.038
N3	−0.077	−0.057	−0.041	−0.075	−0.084	−0.059	−0.082
N4	−0.074	−0.064	−0.041	−0.075	−0.084	−0.059	−0.082
N5	−0.025	0.020	0.056	−0.009	0.025	0.009	−0.038
	24	**26**	**33**	**36**	**36**[b]	**37**	**38**
R1	0.252	0.405	0.533	0.343	0.332	0.329	0.321
N1	−0.296	−0.224	−0.227	−0.290	−0.319	−0.249	−0.242
N2	−0.036	−0.051	−0.035	−0.021	−0.024	−0.067	−0.036
N3	−0.083	−0.139	−0.130	−0.079	−0.071	−0.026	−0.081
N4	−0.083	−0.135	−0.129	−0.079	−0.071	−0.026	−0.081
N5	−0.059	−0.080	−0.039	−0.021	−0.024	−0.067	−0.036

[a] MP2(FC)/6-311 + G(d,p).[68] [b] MP2(FC)/6-31G(d).[68]

compounds are higher than in the neutral molecules. In contrast the transition states all have positive Mulliken charges on N2 and N5 (Table 7); only **19** and **35** have negative charges on N5. The charges on N4 and N5 of the departing N_2 molecule balance out for most compounds, as one would expect. Only in **21**, **26**, **33** and **35** does the eliminated N_2 molecule have a relatively large overall negative (positive) charge. Both compounds have high activation barriers.

Table 7. Mulliken charges of the pentazole ring system and the attached atom for selected transition states.

	2	**13**	**18**	**19**	**19**[a]	**20**	**21**
R1	0.563	0.735	−0.035	0.399	0.334	−0.196	−0.435
N1	−0.436	−0.412	−0.112	−0.334	−0.272	0.135	−0.216
N2	0.102	0.105	0.110	0.060	0.014	0.075	0.085
N3	−0.099	−0.069	−0.039	−0.086	−0.045	−0.045	−0.094
N4	−0.098	−0.076	−0.039	0.050	−0.045	−0.045	0.102
N5	0.046	0.054	0.110	−0.089	0.014	0.075	0.023
	24	**26**	**33**	**35**	**36**	**37**	**38**
R1	0.106	0.396	0.496	–	0.278	0.294	0.263
N1	−0.417	−0.375	−0.353	−0.319	−0.295	−0.305	−0.295
N2	0.089	0.107	0.111	0.009	0.043	0.050	0.037
N3	−0.111	−0.187	−0.168	−0.319	−0.081	−0.070	−0.090
N4	−0.093	−0.156	−0.153	−0.185	−0.058	−0.051	−0.062
N5	0.036	0.009	0.026	−0.185	0.015	0.022	0.009

[a] MP2(FC)/6-311 + G(d,p).[68]

For compounds **2** and **18** we followed the minimum energy path from these transition states along the reaction coordinate in both directions to show that the transition states connect the pentazoles with the corresponding azides (Figures 3 and 4). Compound **2** is representative for the planar transition states of most compounds, and **18** for the nonplanar transition states of **18**–**20**. Figure 4 shows that for the decomposition of **18** the slope of the reaction path towards the pentazole becomes less steep at one point. Essentially, pentazole formation is complete here, and the remaining reaction represents rotation about the N–N bond between the rings to form the minimum structure with an angle of 90° between the ring planes. The small shoulder towards the product side is present because at first both the N1–N5 and N1–N2 distances enlarge as if two dinitrogen molecules (N2N3 and N4N5) were to be eliminated. At the shoulder the N1–N2 distance starts to contract again, and only the N1–N5 bond is broken further down the path. The decomposition of **2** via the calculated transition state proceeds in a straightforward manner and can be used as a model for all planar transition states. As expected from Hammond's postulate,[78, 79] for all cases we found an early transition state that resembles the pentazole system for the strongly exothermic decomposition.

Activation energies: The activation energies for the decomposition reactions are listed in Tables 8–10. Our activation energy for phenylpentazole **36** (MP2: 19.0 kcal mol^{-1}) is in good agreement with previous calculations (19.8 kcal mol^{-1} at the MP2(FC)/6-311G** level).[71] We note that for all compounds the CCSD(T) activation barriers are in general 2–3 kcal mol^{-1} lower than the MP2 activation energies. For the phenylpentazoles we did not obtain coupled cluster values due to computational limitations, but again we expect that these are probably 2–3 kcal lower than the MP2 results. The activation energy of *p*-nitrophenylpentazole (**37**) of 17.8 kcal mol^{-1} is lower than that of phenylpentazole (**36**), and the activation energy of *p*-dimethylaminophenylpentazole (**38**) of 19.5 kcal mol^{-1} is slightly higher than that of **36**, which nicely agrees with experimental observations.[66–68] The

Table 10. Activation energies and reaction energies for the decomposition of the phenylpentazoles to form the corresponding phenylazides and dinitrogen [including zero-point energy correction, in kcal mol^{-1}].

	36	**37**	**38**
E_{act} (MP2)	19.0	17.8	19.5
ΔE_{decomp} (MP2)	−42.8	−45.0	−40.8

Table 8. Activation energies and reaction energies for the decomposition of the pentazoles to form the corresponding azides and dinitrogen [including zero-point energy correction, in kcal mol^{-1}].

	1	**2**	**3**	**4**	**5**	**6**	**7**	**8**	**9**	**10**	**11**	**12**
E_{act} (MP2)	19.2	16.9	19.2	16.4	17.1	18.7	16.5	16.6	15.4	16.2	16.4	16.2
E_{act} (CCSD(T))	16.3	14.5	16.5	14.0	14.4	15.9	13.8	13.5	12.7	13.4	13.4	12.8
ΔE_{decomp} (MP2)	−39.1	−42.5	−39.8	−42.5	−45.2	−41.5	−44.2	−44.8	−43.2	−47.1	−45.8	−45.0
ΔE_{decomp} (CCSD(T))	−32.2	−35.0	−32.4	−35.4	−38.0	−33.7	−36.3	−37.6	−36.3	−38.9	−37.9	−37.1
	13	**14**	**15**	**16**	**17**	**18**	**19**	**20**	**21**	**22**	**23**	**24**
E_{act} (MP2)	14.8	15.8	15.0	14.5	14.9	9.3	16.6	14.2	19.7	11.2	19.2	19.4
E_{act} (CCSD(T))	12.2	12.7	12.0	11.4	11.7	5.2	14.9	6.7	17.4	8.7	16.4	16.1
ΔE_{decomp} (MP2)	−51.1	−48.5	−45.5	−48.4	−50.7	−53.6	−45.0	−47.9	−38.4	−57.5	−39.5	−37.6
ΔE_{decomp} (CCSD(T))	−43.3	−41.3	−38.1	−40.5	−42.6	−45.2	−40.1	−46.7	−31.4	−47.8	−32.2	−30.3

Table 9. Activation energies and reaction energies for the decomposition of the anionic pentazoles to form the corresponding anionic azides and dinitrogen [including zero-point energy correction, in kcal mol^{-1}].

	25	**26**	**27**	**28**	**29**	**30**	**31**	**32**	**33**	**34**	**35**
E_{act} (MP2)	22.9	21.1	22.3	20.7	21.8	20.6	20.2	20.3	20.0	19.7	25.8
E_{act} (CCSD(T))	20.6	18.6	20.0	18.3	19.5	18.0	18.3	17.7	17.9	17.7	23.5
ΔE_{decomp} (MP2)	−23.3	−26.8	−25.1	−29.1	−26.4	−28.1	−30.8	−30.2	−32.8	−34.7	−23.7
ΔE_{decomp} (CCSD(T))	−18.2	−21.6	−19.6	−23.5	−20.3	−22.4	−25.3	−24.1	−26.9	−28.1	−14.4

activation energy for the decomposition of *p*-chlorophenylpentazole (20.8 kcal mol^{-1})[71] and $\Delta G^{\neq}$ for the decomposition of *p*-hydroxyphenylpentazole (19.7 kcal mol^{-1})[70] and tetrabutylammonium *p*-oxophenylpentazole (20.6 kcal mol^{-1}) were obtained from NMR spectroscopic measurements. Also the $\Delta G^{\neq}$ values from B3LYP/6-31 + G(d,p) calculations (*p*-hydroxy: 19.4 kcal, *p*-oxo: 21.3 kcal mol^{-1})[70] are in good agreement with experimental results. We note that the B3LYP values for phenylpentazole (18.4 kcal mol^{-1}) and *p*-nitrophenylpentazole (16.0 kcal mol^{-1})[70] are slightly lower than the calculated MP2 results (19.0 and 17.4 kcal mol^{-1}).

As expected, N_{10} has by far the lowest activation energy (only 5.2 kcal mol^{-1}), so that its detection or isolation is extremely difficult. The MP2 activation energies of the tetrazole tautomers (14.5 and 14.9 kcal mol^{-1}) agree well with previous calculations (14.8 and 15.1 kcal mol^{-1} (MP2(FC)/6-31G(d))[72], but the CCSD(T) values are lower (11.4 and 11.7 kcal mol^{-1}). The activation energy decreases with increasing number of nitrogen atoms in the azole (Figure 5), but

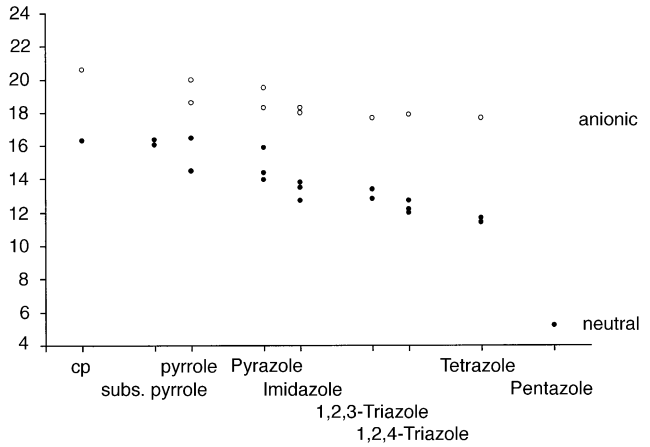

Figure 5. Activation energy for the decomposition of neutral and anionic RN_5 to form the corresponding RN_3 and N_2 (including zero-point energy correction, in kcal mol^{-1}). The compounds shown on the *x* axis are ordered according to increasing number of nitrogen atoms.

there are differences between isomers with the same number of nitrogen atoms and tautomers of these compounds. Imidazolylpentazoles have lower activation barriers than pyrazolylpentazoles, and 1,2,3-triazoles have higher activation barriers than 1,2,4-triazoles. The 2*H* tautomers have higher activation barriers than the 1*H* tautomers. Amino substitution of **2** increases the activation energy from 14.5 kcal mol^{-1} to 16.4 and 16.1 kcal mol^{-1}. While there is a large difference in the activation energies of **2** (14.5 kcal mol^{-1}) and **3** (16.5 kcal mol^{-1}), the position at which an amino group is attached does not influence the activation energy significantly.

The cyclopentadienyl anion **25** (20.6 kcal mol^{-1}) has a higher activation energy than all the other anions with nitrogen atoms in the ring system. The neutral cyclopentadienylpentazole **1** also has a high activation energy (16.3 kcal mol^{-1}) compared to the azole compounds, considering that cyclopentadiene is not an aromatic system. Compared to the phenylpentazoles, the anionic compounds all have higher activation energies than *p*-dimethylaminophenylpentazole (**38**), which is stable up to 50 °C.[66] The neutral azoles have lower activation energies than the nitro compound **37**, which has not been isolated yet due to its instability.[68] Pentazole (**19**), fluoropentazole (**20**) and cyanopentazole (**22**) have activation energies of 14.9, 6.7 and 8.7 kcal mol^{-1}, respectively, but methylpentazole has an activation energy of 17.4 kcal mol^{-1} (19.7 kcal mol^{-1} at MP2), which is higher than that of **38**. The pentazole anion (**35**) has the highest activation energy for decomposition of 23.5 kcal mol^{-1} (CCSD(T)/aug-cc-pVTZ: 27.7 kcal mol^{-1}).[19]

Decomposition energies: The energy released on decomposition is an important factor in the design of high-energy materials. An increase in the released energy enhances the performance of a highly energetic system. Like the activation energy, the decomposition energy is related to the number of nitrogen atoms in the azolylpentazoles. The decomposition becomes more exothermic with increasing number of nitrogen atoms in the system and with an increase in electron-withdrawing character of the azole (Figure 6). It is less

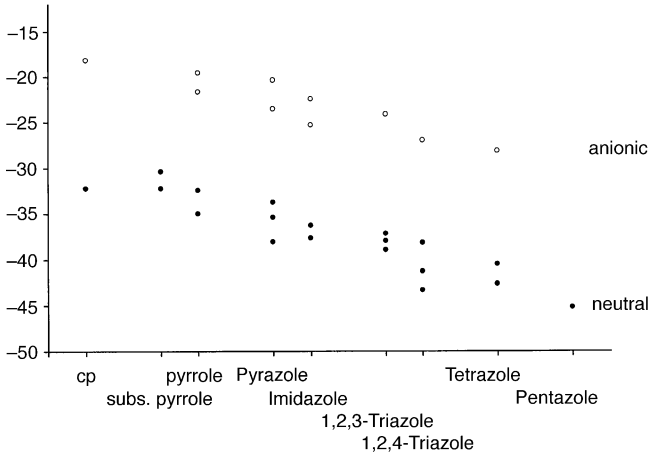

Figure 6. Reaction energy for the decomposition of neutral and anionic RN_5 to form the corresponding RN_3 and N_2 (including zero-point energy correction, in kcal mol^{-1}). The compounds shown on the *x* axis are ordered according to increasing number of nitrogen atoms.

exothermic for the anions, as mentioned above. As expected from Hammond's postulate, the activation energy for decomposition and the decomposition energy (see Figure 7) are nicely correlated (correlation coefficient: 0.80); a more exothermic reaction is accompanied by a lower activation barrier. The activation energy increases with decreasing number of nitrogen atoms in the azole and with increasing electron-donating character of the azole. The anionic compounds, therefore, have higher activation energies (17.7–18.6 kcal mol^{-1}) and lower decomposition energies than the corresponding neutral compounds (activation energies: 11.4–16.5 kcal mol^{-1}).

The highest decomposition energies are found for N_{10} (**18**; −45.2 kcal mol^{-1}), fluoropentazole (**20**; −46.7 kcal mol^{-1}) and cyanopentazole (**22**; −47.8 kcal mol^{-1}). The CCSD(T) values here are generally 7 kcal mol^{-1} below the MP2 values, with **20** and **22** as exceptions. The cyclopentadienyl anion **25** has the lowest decomposition energy (−18.2 kcal mol^{-1}) of all the

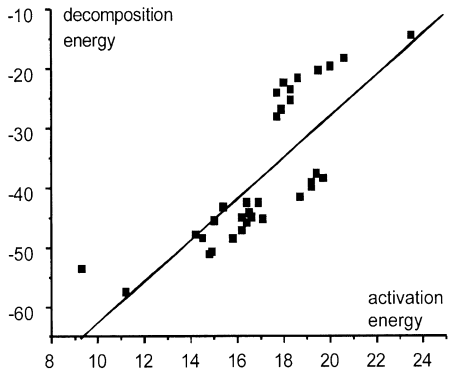

Figure 7. Correlation between activation energy and decomposition energy (CCSD(T) values, in kcal mol^{-1}).

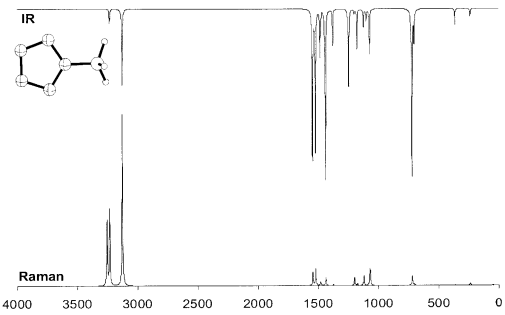

Figure 8. Calculated vibrational spectrum of methylpentazole (in cm^{-1}).

substituted anionic pentazoles. The decomposition energies of all anions and of the cyclopentadienyl compound **1** at the MP2 level are less exothemic than that of *p*-dimethylaminophenylpentazole (**38**). The other neutral azolylpentazoles have decomposition energies between -32.4 and -45.2 kcal mol^{-1} for N_{10} (**18**). Methylpentazole **21** has a low decomposition energy of only -31.4 kcal mol^{-1}. Pentazole, fluoropentazole, and cyanopentazole have high decomposition energies of -40.1, -46.4 and -47.8 kcal mol^{-1}. In contrast, the pentazole anion has the lowest decomposition energy of only -14.4 kcal mol^{-1} (14.3 kcal mol^{-1} at the CCSD(T)/aug-cc-pVTZ level[19]). For most anions the activation energy is in the same range as the absolute value of the decomposition energy.

In the synthesis of pentazole compounds, azide ions are added to a solution containing a diazonium salt, generated by diazotation of an amine. Such a synthesis of the pentazole ion (**35**) would require N_2, which is inert, and the pentazole (**19**) would require HN_2^+, which is not available. For all other compounds at least the corresponding amines for diazotation are known, and some of them are commercially available. Apart from NCN_2^+, the synthesis of the diazonium compounds from the amines should not be a problem. For the synthesis of methylpentazole (**21**), we suggest the reaction of diazomethane and HN_3, which are both very volatile. Since methylpentazole should also be volatile, like all small methyl compounds, it should be possible to perform this reaction in the gas phase, at low concentrations to make the hazardous reaction safer. The calculated vibrational spectra of methylpentazole are shown in Figure 8 for the purpose of future identification of this material. The most intense absorption in the IR spectrum is the CN stretching mode. In the Raman spectrum the CH stretching modes give the most intense signals.

NMR chemical shifts: ^{15}N NMR chemical shifts of cesium/TMA pentazolylphenolate [$\delta = -81.1$ (N1), -29.7 (N3/N4), 1.9 ppm (N2/N5)][7] and of *p*-dimethylaminophenyl- in $CDCl_3$ [$\delta = -80.0$ (N1), -27.1 (N2/N5), $+4.9$ ppm (N3/N4)],[69] *p*-oxophenyl- in CD_3OD/D_2O [$\delta = -28.7$ (N2/5), 3.6 ppm (N3/N4)],[70] *p*-chlorophenyl- in CD_3OD/D_2O [$\delta = -82.7$ (N1)],[71] *p*-methoxyphenyl- in CD_2Cl_2 [$\delta = -28.1$ ppm (N2/N5)],[48] *p*-hydroxyphenyl [$\delta = -81.6$ ppm (N1), -27.6 (N2/N5), 4.2 ppm (N3/N4)][7] and tetrazolylpentazole in CH_3OH/Et_2O [$\delta = -29.7$ (N2/N5), 7.7 ppm (N3/N4)][72] are known. B3LYP-GIAO calculations on alkali and alkaline earth metal salts of N_5^-[48] show that the ^{15}N NMR resonances of the pentazole ring are spread over a broad range ($\delta = +17.6$ to -96.1 ppm for N1), and the calculated values for phenylpentazole compounds are in good agreement with experimental values mentioned above. For easier identification of the not-yet-synthesized pentazole compounds we calculated the ^{15}N NMR spectra of all investigated compounds (Table 11). The calculated ^{15}N NMR spectrum of **38** is in good agreement with the experimental values for N1 and N2. The N3 value is slightly different, which may be due to solvent effects.[80] The NMR data of the azolylpentazoles must be interpreted with caution because of the acidity of the azoles.[73] For these compounds it is very difficult to determine the equilibrium between the different tautomers and the anion in solution, and to include the effect of the solvent. Certainly the difference between protonated and unprotonated N1/N4 and N2/N3 would be significant, and solution values may be quite different. The experimental data for tetrazolylpentazole suggest a more anionic structure in solution, which agrees with the acidity of tetrazoles. The azolylpentazoles generally have a lower N1 shift than their anions. The N2 shift is just below zero and the N3 shift just above zero. The alkylpentazoles **21** and **22** show larger N1 shifts ($\delta = -100.4$ and -122.5 ppm, respectively) than the phenylpentazoles.

Conclusion

Five-membered aromatic rings containing nitrogen atoms (azoles) form pentazole compounds with activation energies for decomposition of up to 16.5 kcal mol^{-1} for neutral compounds and 20.0 kcal mol^{-1} for anionic tetrazolylpentazolates. The activation energy of their decomposition and the decomposition energy are related to the electron-donating character of the azole. The activation energy decreases and the decomposition energy increases with increasing number of nitrogen atoms. Removal of a proton from the acidic azolylpentazoles leads to anionic compounds that are more stable than the corresponding neutral compounds, some of which have higher activation energies and lower decomposition energies than *p*-dimethylaminophenylpentazole, one of the most stable and best investigated pentazole compounds known.

Table 11. Calculated GAIO-B3LYP ^{15}N NMR shifts relative to CH_3NO_2.

	1	2	3	4	5	6	7	8	9	10	11	12	13	14
N1	−90.8	−91.6	−89.1	−96.3	−92.2	−94.4	−119.5	−90.2	−92.2	−101.1	−97.2	−96.4	−97.1	−97.5
N2	−6.3	−32.3	−22.4	−25.7	−9.4	−20.3	−64.0	−10.9	−26.0	−22.1	−10.3	−10.8	−20.6	−2.6
N3	23.9	18.7	21.8	23.3	26.0	23.4	−17.4	25.7	22.2	25.9	27.7	27.4	26.4	25.2
N4	23.9	21.9	20.7	24.4	25.8	23.0	−14.2	24.2	25.2	27.1	27.0	26.1	27.3	26.7
N5	−6.3	−25.1	−20.5	−19.3	−11.1	−19.1	−57.9	−14.7	−16.7	−17.3	−12.4	−14.4	−12.6	−2.8
	15	**16**	**17**	**18**	**19**	**19**[a]	**20**	**21**	**22**	**23**	**24**	**25**	**26**	**27**
N1	−97.8	−103.3	−103.7	−103.5	−119.7	−113.8	−60.6	−100.4	−122.5	−88.7	−88.3	−70.0	−70.3	−73.3
N2	−13.7	−17.6	−3.4	−4.5	−13.6	−19.9	−33.4	−7.5	3.1	−23.4	−21.0	−40.8	−28.6	−37.1
N3	28.3	29.5	28.5	32.2	23.3	15.4	25.3	27.5	30.4	21.1	18.7	2.2	7.6	4.9
N4	24.5	30.7	29.3	31.9	23.3	15.4	25.3	27.5	30.4	20.1	18.9	2.4	6.1	3.6
N5	−22.8	9.8	−3.1	−4.2	−13.6	−19.9	−33.4	−7.5	3.1	−20.7	−26.5	−40.9	−31.9	−37.5
	28	**29**	**30**	**31**	**32**	**33**	**34**	**35**	**35**[a]	**36**	**37**	**38**	**38** (exptl)[b]	
N1	−75.1	−77.3	−74.0	−72.2	−79.3	−77.2	−82.7	3.9	−3.5	−81.2	−84.8	−81.4	−80.0	
N2	−20.5	−33.7	−25.7	−13.0	−19.4	−7.8	−5.8	3.9	−3.5	−15.9	−13.6	−19.9	−21.1	
N3	11.6	6.5	9.3	11.1	12.7	13.0	14.8	3.9	−3.5	26.6	29.3	23.9	+4.9	
N4	9.6	6.6	8.4	11.1	11.0	13.4	15.0	3.9	−3.5	26.6	29.3	23.8	+4.9	
N5	−23.8	−33.7	−28.4	−13.0	−22.8	−8.8	−6.0	3.9	−3.5	−15.9	−13.6	−20.2	−21.1	

[a] B3LYP/6−31+G**.[70] [b] $CDCl_3$.[69]

Fluoropentazole and cyanopentazole, which both have electron-withdrawing substituents on the pentazole ring, are not very stable. Together with dipentazole N_{10} they have different transition states than the other compounds. A decomposition path for dipentazole N_{10}, which is the least stable of all investigated pentazoles, to form pentazole azide and dinitrogen was found. In contrast, the nonaromatic cyclopentadienylpentazole and methylpentazole are remarkably stable, the activation energy for the decomposition of methylpentazole being higher than that for *p*-dimethylaminophenylpentazole. A possible path for the synthesis of methylpentazole and its calculated vibrational spectra were discussed.

Methods of Calculation

The geometries of all compounds were optimized at the MP2 level (full active orbital space) within the symmetry constraints stated in the respective tables using a 6-311G(d) basis set.[81] Vibrational frequencies were computed at the optimized structures. All pentazoles and azides were true minima on the potential energy surface with no imaginary frequencies. The located transition states were first-order with Cartesian displacement coordinates of the imaginary frequency mode corresponding to the formation of nitrogen and an azide from the pentazole compound. For further validation, single-point CCSD(T) calculations using an augmented cc-pVDZ basis set[82] keeping the carbon and nitrogen 1s electrons as frozen (FC) were performed.[83] An NBO analysis gave basically the same charge distribution as a Mulliken analysis, and the latter method is therefore used in the discussion.

GIAO isotropic chemical shifts relative to CH_3NO_2 were calculated for all pentazoles using the B3LYP functional with a 6-311+G(2d,p) basis set at the MP2(6-311G(d)) geometries. We note that in a similar study the calculated values correlated nicely with the experimental data according to the linear equation $\sigma_{exptl} = 1.0683\,\sigma_{calcd} - 4.70$.[48]

Acknowledgement

This work was supported by the Alexander von Humboldt Foundation (Bonn) and the Auckland University Research Committee. We thank the referees for helpful comments.

[1] D. E. Chavez, M. A. Hiskey, R. D. Gilardi, *Angew. Chem.* **2000**, *112*, 1861–1863; *Angew. Chem. Int. Ed.* **2000**, *39*, 1791–1793.
[2] A. Hammerl, G. Holl, M. Kaiser, T. M. Klapötke, H. Nöth, U. Ticmanis, M. Warchhold, *Inorg. Chem.* **2001**, *40*, 3570–3575.
[3] K. O. Christe, W. W. Wilson, J. A. Sheehy, J. A. Boatz, *Angew. Chem.* **1999**, *111*, 2112–2117, *Angew. Chem. Int. Ed.* **1999**, *38*, 2004–2009.
[4] A. Vij, W. W. Wilson, V. Vij, F. S. Tham, J. A. Sheehy, K. O. Christe, *J. Am. Chem. Soc.* **2001**, *123*, 6308–6313.
[5] R. J. Bartlett, *Chem. Ind.* **2000**, 140–143, and references therein; a compilation of data for N_2 to N_{10} can be found at http://www.qtp.u-fl.edu/~bartlett/polynitrogen.pdf.
[6] T. M. Klapötke, *Angew. Chem.* **1999**, *111*, 2694–2696; *Angew. Chem. Int. Ed.* **1999**, *38*, 2536–2538, and references therein.
[7] A. Vij, J. G. Pavlovich, W. W. Wilson, V. Vij, K. O. Christe, *Angew. Chem.* **2002**, *114*, 3177–3180; *Angew. Chem. Int. Ed.* **2002**, *41*, 3051–3054.
[8] F. Cacace, G. de Petris, A. Troiani, *Science* **2002**, *295*, 480–481.
[9] F. Cacace, *Chem. Eur. J.* **2002**, *8*, 3839–3847.
[10] P. Pyykkö, N. Runeberg, *J. Mol. Struct. (THEOCHEM)* **1991**, *234*, 279–290.
[11] J. Wasilewski, *J. Chem. Phys.* **1996**, *105*, 10969–10982.
[12] A. A. Korkin, A. Balkova, R. J. Bartlett, R. J. Boyd, P. von R. Schleyer, *J. Phys. Chem.* **1996**, 5702–5714.
[13] M. N. Glukhovtsev, H. Jiao, P. von R. Schleyer, *Inorg. Chem.* **1996**, *35*, 7124–7133.
[14] W. J. Lauderdale, J. F. Stanton, R. J. Bartlett, *J. Phys. Chem.* **1992**, *96*, 1173–1178.
[15] J. P. Zheng, J. Waluk, J. Spanget-Larsen, D. M. Blake, J. G. Radziszewski, *Chem. Phys. Lett.* **2000**, *328*, 227–233.
[16] S. A. Perera, R. J. Bartlett, *Chem. Phys. Lett.* **1999**, *314*, 381–387.
[17] H. Östmark, O. Launilla, S. Wallin, R. Tryman, *J. Raman Spectrosc.* **2001**, *32*, 195–199.
[18] X. Wang, H. R. Hu, A. Tian, N. B. Wong, S.-H. Chien, W.-K. Li, *Chem. Phys. Lett.* **2000**, *329*, 483–489.
[19] M. T. Nguyen, T.-K. Ha, *Chem. Phys. Lett.* **2001**, *335*, 311–320.
[20] R. Engelke, *J. Phys. Chem.* **1992**, *96*, 10789–10792.
[21] T. M. Klapötke, *J. Mol. Struct.* (*THEOCHEM)* **2000**, *499*, 99–104.
[22] M. Tobita, R. J. Bartlett, *J. Phys. Chem. A* **2001**, *105*, 4107–4113.
[23] M. N. Glukhovtsev, P. von R. Schleyer, *Chem. Phys. Lett.* **1992**, *198*, 547–554.
[24] Q-S. Li, X-G. Hu, W.-G. Xu, *Chem. Phys. Lett.* **1998**, *287*, 94–99.
[25] X. Wang, Y. Ren, M. B. Shuai, *J. Mol. Struct. (THEOCHEM)* **2001**, *538*, 145–156.
[26] X. Wang, A. M. Tian, N. B. Wong, C. K. Law, W. R. Li, *Chem. Phys. Lett.* **2001**, *338*, 367–374.
[27] L. J. Wang, S. Li, Q. S. Li, *J. Comput. Chem.* **2001**, *22*, 1334–1339.

[28] L. Gagliardi, G. Orlandi, S. Evangelisti, B. O. Roos, *J. Chem. Phys.* **2001**, *114*, 10733–10737.
[29] G. Chung, M. W. Schmidt, M. S. Gordon, *J. Phys. Chem. A* **2000**, *104*, 5647–5650.
[30] J. Kortus, M. R. Pederson, S. L. Richardson, *Chem. Phys. Lett.* **2001**, *340*, 565–570.
[31] L. Gagliardi, S. Evangelisti, A. Bernhardsson, R. Lindh, B. O. Roos, *Int. J. Quantum Chem.* **2000**, *77*, 311–315.
[32] T. M. Klapötke, R. D. Harcourt, *J. Mol. Struct. (THEOCHEM)* **2001**, *541*, 237–242.
[33] M. T. Nguyen, T.-K. Ha, *Chem. Ber.* **1996**, *129*, 1157–1159.
[34] C. Chen, *Int. J. Quantum Chem.* **2000**, *80*, 27–37.
[35] Q. S. Li, L. J. Wang, *J. Phys. Chem. A* **2001**, *105*, 1203–1207.
[36] M. R. Manaa, *Chem. Phys. Lett.* **2000**, *331*, 262–268.
[37] H. H. Michels, J. A. Montgomery, Jr., K. O. Christe, D. D. Dixon, *J. Phys. Chem.* **1997**, 20, 187–194.
[38] T. M. Klapötke, A. Schulz, *Main Group Met. Chem.* **1997**, *20*, 335–338.
[39] K. F. Ferris, R. J. Bartlett, *J. Am. Chem. Soc.* **1992**, *114*, 8302–8303.
[40] G. A. Olah, G. K. S. Prakash, G. Rasul, *J. Am. Chem. Soc.* **2001**, *123*, 3308–3310.
[41] Y. Ren, X. Wang, N. B. Wong, *Int. J. Quantum Chem.* **2001**, *82*, 34–43.
[42] T.-K. Ha, O. Suleimenov, M. T. Nguyen, *Chem. Phys. Lett.* **1999**, *315*, 327–334.
[43] Z. Tang, J. J. Belbruno, R. Huang, L. Zheng, *J. Chem. Phys.* **2000**, *112*, 9276–9281.
[44] M. T. Nguyen, M. A. McGinn, A. F. Hegarty, *Polyhedron* **1985**, *4*, 1721–1726.
[45] S. Inagaki, N. Goko, *J. Am. Chem. Soc.* **1987**, *109*, 3234–3240.
[46] J. Catalan, J. L. G. De Paz, M. Yanez, J. Elguero, *Chem. Scripta* **1984**, *24*, 84–91.
[47] M. N. Glukhovtsev, P. von R. Schleyer, C. Marker, *J. Phys. Chem.* **1993**, *97*, 8200–8206.
[48] L. A. Burke, R. N. Butler, J. C. Stephens, *J. Chem. Soc. Perkin Trans. 2* **2001**, 1679–1684.
[49] G. Frenking, *J. Organomet. Chem.* **2001**, *635*, 9–23.
[50] M. Lein, J. Frunzke, A. Timoshkin, G. Frenking, *Chem. Eur. J.* **2001**, *7*, 4155–4163.
[51] L. Gagliardi, P. Pyykkö, *J. Am. Chem. Soc.* **2001**, *123*, 9700–9701.
[52] L. Gagliardi, P. Pyykkö, *J. Phys. Chem. A* **2002**, *106*, 4690–4694.
[53] S. I. Kotelevskij, O. V. Prezhdo, *Tetrahedron* **2001**, *57*, 5715–5729.
[54] M. K Cyranski, T. M. Krygowski, A. R. Kartritzky, P. von R. Schleyer, *J. Org. Chem.* **2002**, *67*, 1333–1338, and references therein.
[55] G. P. Bean, *J. Org. Chem.* **1998**, *63*, 2497–2506.
[56] R. J. Doerksen, A. J. Thakkar, *J. Phys. Chem. A* **1999**, *103*, 10009–10014.
[57] S.Fau, R. J. Bartlett, *J. Phys. Chem. A* **2001**, *105*, 4096–4106.
[58] S. Fau, K. J. Wilson, R. J. Bartlett, *J. Phys. Chem. A* **2002**, *106*, 4639–4644.
[59] L. J. Wang, Q. S. Li, P. Warburton, P. G. Mezey, *J. Phys. Chem. A* **2002**, *106*, 1872–1876.
[60] R. D. Harcourt, T. M. Klapötke, *Z. Naturforsch. B* **2002**, *57*, 983–992.
[61] K. Clusius, H. Hürzeler, *Helv. Chim. Acta* **1954**, *37*, 798.
[62] R. Huisgen, I. Ugi, *Angew. Chem.* **1956**, *68*, 705–706; R. Huisgen, I. Ugi, *Chem. Ber.* **1957**, *90*, 2914–2927.
[63] I. Ugi, *Angew. Chem.* **1961**, *73*, 172.
[64] J. D. Wallis, J. D. Dunitz, *J. Chem. Soc. Chem. Commun.* **1983**, 910–911.
[65] F. Biesemeier, U. Müller, W. Massa, *Z. Anorg. Allg. Chem.* **2002**, *628*, 1933–1934.
[66] I. Ugi, R. Huisgen, *Chem. Ber.* **1958**, *91*, 531–537.
[67] I. Ugi, H. Perlinger, L. Behringer, *Chem. Ber.* **1958**, *91*, 2324–2329.
[68] R. N. Butler, S. Collier, A. F. M. Fleming, *J. Chem. Soc. Perkin. Trans. 2* **1996**, 801–803.
[69] R. Müller, J. D. Wallis, W. von Phillipsborn, *Angew. Chem.* **1985**, *97*, 515–517; *Angew. Chem. Int. Ed. Engl.* **1985**, *24*, 513–515.
[70] V. Benin, P. Kaszynski, J. G. Radzisewski, *J. Org. Chem.* **2002**, *67*, 1354–1358.
[71] R. N. Butler, A. Fox, S. Collier , L. A. Burke, *J. Chem. Soc. Perkin Trans. 2*, **1998**, 2243–2247.
[72] A. Hammerl, T. M. Klapötke, *Inorg. Chem.* **2002**, *41*, 906–912.
[73] J. Catalán, J. Palomar, J. L. G. de Paz, *Int. J. Mass. Spectrom. Ion Process.* **1998**, *175*, 51–59.
[74] S. C. S. Bugalho, E. M. S. Maçôas, M. L. S. Cristiano, R. Fausto, *Phys. Chem. Chem. Phys.* **2001**, *3*, 3541–3547.
[75] R. N. Butler, V. C. Garvin, H. Lumbroso, C. Lièbeois, *J. Chem. Soc. Perkin Trans. 2* **1984**, 721–725.
[76] A. P. Mazurek, N. Sadlej-Sosnowska, *Chem. Phys. Lett.* **2000**, *330*, 212–218.
[77] R. Goddard, O. Heinemann, C. Krüger, *Acta. Cryst. C* **1997**, *53*, 590–592, and references therein.
[78] G. S. Hammond, *J. Am. Chem. Soc.* **1955**, *77*, 334–338.
[79] G. Lendvay, *J. Phys. Chem.* **1994**, *98*, 6098–6104.
[80] M. Witanowski, L. Stefaniak, G. A. Webb in *Annual Reports on NMR Spectroscopy* **1993**, *25* (Ed. G. A. Webb), Academic Press, London, pp. 86–87.
[81] Gaussian 98, Revision A.8, M. J. Frisch, G. W. Trucks, H. B. Schlegel, G. E. Scuseria, M. A. Robb, J. R. Cheeseman, V. G. Zakrzewski, J. A. M. Jr., R. E. Stratmann, J. C. Burant, S. Dapprich, J. M. Millam, A. D. Daniels, M. C. S. K. N. Kudin, O. Farkas, J. Tomasi, V. Barone, M. Cossi, R. Cammi, B. Mennucci, C. Pomelli, C. Adamo, S. Clifford, J. Ochterski, G. A. Petersson, P. Y. Ayala, Q. Cui, K. Morokuma, D. K. Malick, A. D. Rabuck, K. Raghavachari, J. B. Foresman, J. Cioslowski, J. V. Ortiz, A. G. Baboul, B. B. Stefanov, G. Liu, A. Liashenko, P. Piskorz, I. Komaromi, R. Gomperts, R. L. Martin, D. J. Fox, T. Keith, M. A. Al-Laham, C. Y. Peng, A. Nanayakkara, C. Gonzalez, M. Challacombe, P. M. W. Gill, B. Johnson, W. Chen, M. W. Wong, J. L. Andres, C. Gonzalez, M. Head-Gordon, E. S. Replogle, J. A. Pople, Pittsburgh PA, **1998**.
[82] D. E. Woon, T. H. Dunning, Jr., *J. Chem. Phys.* **1993**, *98*, 1358–1371.
[83] MOLPRO, a package of ab initio programs designed by H.-J.Werner and P. J. Knowles, version 2002.3, R. D. Amos, A. Bernhardsson, A. Berning, P. Celani, D. L. Cooper, M. J. O. Deegan, A. J. Dobbyn, F. Eckert, C. Hampel, G. Hetzer, P. J. Knowles, T. Korona, R. Lindh, A. W. Lloyd, S. J. McNicholas, F. R. Manby, W. Meyer, M. E. Mura, A. Nicklass, P. Palmieri, R. Pitzer, G. Rauhut, M. Schütz, U. Schumann, H. Stoll, A. J. Stone, R. Tarroni, T. Thorsteinsson, H.-J. Werner.
[84] J. J. P. Stewart, *J. Comput. Chem.* **1989**, *10*, 209–264.

Received: May 12, 2003 [F5125]

